Lasing in Non-Hermitian Flat Bands: Quantum Geometry, Coherence, and the Fate of Kardar-Parisi-Zhang Physics

Ivan Amelio[1] and Nathan Goldman[1,2]
[1]Center for Nonlinear Phenomena and Complex Systems, Université Libre de Bruxelles, CP 231, Campus Plaine, B-1050 Brussels, Belgium
[2]Laboratoire Kastler Brossel, Collège de France, CNRS, ENS-Université PSL, Sorbonne Université, 11 Place Marcelin Berthelot, 75005 Paris, France

(Received 18 August 2023; revised 3 April 2024; accepted 8 April 2024; published 1 May 2024)

We show that lasing in flat-band lattices can be stabilized by means of the geometrical properties of the Bloch states, in settings where the single-particle dispersion is flat in both its real and imaginary parts. We illustrate a general projection method and compute the collective excitations, which display a diffusive behavior ruled by quantum geometry through a peculiar coefficient involving gain, losses and interactions, and entailing resilience against modulational instabilities. Then, we derive an equation of motion for the phase dynamics and identify a Kardar-Parisi-Zhang term of geometric origin. This term is shown to exactly cancel whenever the real and imaginary parts of the laser nonlinearity are proportional to each other, or when the uniform-pairing condition is satisfied. We confirm our results through numerical studies of the π-flux diamond chain. This Letter highlights the key role of Bloch geometric effects in nonlinear dissipative systems and KPZ physics, with direct implications for the design of laser arrays with enhanced coherence.

DOI: 10.1103/PhysRevLett.132.186902

Introduction.—The physics of weakly dispersive bands, where correlation effects and interactions dominate over kinetic energy, has been the topic of various conceptual and experimental studies, starting from the strong coupling limit of the Hubbard model and the fractional quantum Hall effect, and pioneering, in recent years, the discovery of flat bands in twisted bilayer graphene [1] and the consequent experimental observation of superconductivity [2] and correlated insulators [3]. The most appealing flat bands are the ones displaying a complex structure of the Bloch states, not ascribable to a trivial atomic limit. The crucial role of Bloch state geometry for (quasi)condensation [4–6] and superfluid transport [7,8] is now well established.

Similarly to weakly interacting atomic BECs in flat bands [6,9], it is natural to consider lasing in flat band systems within a semiclassical framework. However, in such a non-Hermitian context, one should specify whether the flatness condition applies to the real or imaginary part of the single-particle dispersion relation. In this Letter, we explore the situation where the Bloch geometry stabilizes a lasing state *in a purely nonlinear fashion*, due to gain competition. This goes beyond a series of recent works on topological lasers [10,11] and polariton condensation on the Lieb lattice [12], where a privileged Bloch state benefits from a larger gain or quality factor *already at the linear level*. In other words, this Letter considers single-particle bands that are flat both in their real and imaginary parts.

This Letter also addresses a question that is specifically relevant to nonequilibrium quasicondensates: the fate of Kardar-Parisi-Zhang (KPZ) physics [13–16] in a flat band. Indeed, in dispersive systems the KPZ nonlinearity is proportional to the bandwidth. Here, we determine under which conditions the KPZ nonlinearity survives in non-Hermitian flat bands, revealing the key role of Bloch geometry in this context.

We start by introducing the semiclassical lasing equations on the diamond chain, as well as a real-space projection method to the lowest flat band. The geometry of the Bloch states determines the steady-state lasing mode and the collective modes, calculated by the Bogoliubov method. In particular, the onset of modulational instabilities is shown to be hindered by quantum geometry. We then go beyond Bogoliubov, by introducing stochastic noise and allowing for large phase fluctuations. Adiabatically eliminating density fluctuations yields an equation for the phase featuring a nonlinear KPZ term, which is proportional to a Bloch geometric constant. This term is shown to cancel out whenever the real part of the laser nonlinearity is proportional to the imaginary part, or when the uniform-pairing condition is satisfied. Our results are confirmed by numerical simulations. Finally, we discuss connections with previous works on flat bands [12,17,18] and outline future directions.

Model and projection.—We consider lasing in a semiclassical framework, particularly adequate for lattices of microring laser resonators [19], exciton-polariton micropillars [20], and VCSEL's arrays [21]. The light field (or polariton field, in the micropillar case) $\psi_{x\sigma}(t)$, is defined on a lattice, where σ denotes one of the N_σ orbitals within the xth unit cell, N_x being the number of unit cells. We assume that the field obeys a complex Ginzburg-Landau equation (CGLE) [22]

$$i\partial_t\psi_{x\sigma} = (H_0\psi)_{x\sigma} + \frac{i}{2}[(1-i\alpha)r_{x\sigma} - \gamma]\psi_{x\sigma}, \quad (1)$$

$$\partial_t r_{x\sigma} = \gamma_R P - \gamma_R(1 + |\psi_{x\sigma}|^2/n_S)r_{x\sigma}, \quad (2)$$

where the reservoir of carriers is described by the local gain strength $r_{x\sigma}$, and the Henry factor α [23] sets the relative strength of the interaction (aka refractive index in the laser context) over gain nonlinearities. Furthermore, P and γ are, respectively, gain and losses, which we assume to be uniform along the system, n_S is the saturation density that determines the strength of gain competition. While a slow carrier dynamics can potentially give rise to further instabilities [11,17,24,25], we assume that the reservoir relaxation rate γ_R represents the fastest scale, such that the adiabatic approximation holds:

$$i\partial_t\psi_{x\sigma} = (H_0\psi)_{x\sigma} + \frac{i}{2}\left[(1-i\alpha)\frac{P}{1+|\psi_{x\sigma}|^2/n_S} - \gamma\right]\psi_{x\sigma}. \quad (3)$$

The single-particle Hamiltonian H_0 encodes the hopping on the lattice. Because of the relevance of 1D lattices for KPZ physics, we will henceforth consider the π-flux diamond chain, a 1D setting displaying flat bands [26]. However, we expect our analytical results to hold for other models and independently of the dimensionality of the system. The diamond chain is sketched in Fig. 1 and is described by the quadratic Hamiltonian

$$H_0 = -J\sum_{x=1}^{N_x}(c_x^* a_x - b_x^* a_x + i a_{x+1}^* b_x + i a_{x+1}^* c_x) + \text{H.c.}, \quad (4)$$

where σ runs over A, B, C and we denoted $a \equiv \psi_{xA}$, $b \equiv \psi_{xB}, c \equiv \psi_{xC}$. We emphasize that each plaquette contains a π flux, which is key to form flat bands [26]; for the sake of notations, we have chosen a gauge in which lasing occurs in the zero-momentum Bloch state. Such Hamiltonian can be implemented in lattices of microring laser resonators with passive dielectric elements [27,28] or polaritons micropillars in an external magnetic field [29], as well as in superconducting qubits [30].

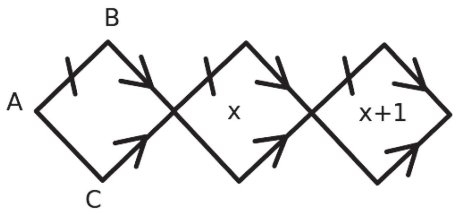

FIG. 1. Sketch of the diamond chain, with three inequivalent sites A, B, C per unit cell. The dashed on the link stands for a minus sign in the hopping amplitude, the arrow for a $+i$.

Under periodic boundary conditions, the energy spectrum associated with H_0 yields three perfectly flat bands, with energies $\{-2J, 0, 2J\}$. From now on, we assume that all the dynamics occurs in the lowest band, requiring the hopping J to dominate over all other scales in the problem (P, γ and interactions). The Bloch eigenstates corresponding to this band have the form $u_k(\sigma) = [1/(2\sqrt{2})](2, -1 - ie^{ik}, 1 - ie^{ik})^T$, where k denotes the quasimomentum. For a given field configuration, its projection onto the lowest band has the form $(\mathbb{P}\psi)_{x\sigma} = \sum_k u_k(\sigma)(e^{ikx}/\sqrt{N_x})\bar{\psi}_k$. Fourier transforming the coefficients $\bar{\psi}_k$ yields the auxiliary field $\bar{\psi}_x$, which is the relevant representation used in the following.

To tackle the problem, we assume that density fluctuations are small on top of a noiseless steady-state ψ^{ss}, with uniform density along x, $\rho_\sigma = |\psi^{ss}_{x\sigma}|^2/n_S$. In this way we can expand the nonlinearity as

$$\frac{1}{1+|\psi_{x\sigma}|^2/n_S} \simeq \frac{1+2\rho_\sigma}{(1+\rho_\sigma)^2}\left[1 - \frac{|\psi_{x\sigma}|^2/n_S}{1+2\rho_\sigma}\right]. \quad (5)$$

This leads to a cubic CGLE with *site-dependent* interaction coefficients. We use the convolution

$$(\mathbb{P}\psi)_{x\sigma} = \frac{1}{N_x}\sum_{k,y} u_k(\sigma)e^{ik(x-y)}\bar{\psi}_y \quad (6)$$

(which makes the nonlocality introduced by the projection explicit) to obtain

$$i\partial_t\bar{\psi}_x = \left(-2J - i\frac{\gamma}{2}\right)\bar{\psi}_x + i\frac{P}{2}\sum_y K^\rho(x,y)\bar{\psi}_y - \frac{iP}{2n_S}(1-i\alpha)\sum_{y_1y_2y_3} K^\rho(x,y_1,y_2,y_3)\bar{\psi}^*_{y_1}\bar{\psi}_{y_2}\bar{\psi}_{y_3}, \quad (7)$$

where we have defined the "quantum geometric kernel"

$$K^\rho(x,y_1,y_2,y_3) = \sum_{k_1k_2k_3}\frac{e^{ik_1z_1 - ik_2z_2 - ik_3z_3}}{N_x^3}\Lambda^\rho(k_1,k_2,k_3). \quad (8)$$

Here, we used the shortcut $z_j \equiv y_j - x$ and introduced the crucial object

$$\Lambda^\rho(k_1,k_2,k_3) = \sum_\sigma \frac{u^*_{k_2+k_3-k_1}(\sigma)u^*_{k_1}(\sigma)u_{k_2}(\sigma)u_{k_3}(\sigma)}{(1+\rho_\sigma)^2}, \quad (9)$$

which contains the geometric properties of the Bloch states. Generalization to other functional forms of the nonlinearity is straightforward. In particular, lasing near threshold corresponds to the limit $\rho_\sigma \to 0$. In this case, if $u_k = u^*_{-k}$, and under the uniform density assumption $|u_0(\sigma)|^2 = (1/N_\sigma)$, the quantity $\sqrt{1-|\Lambda^0(k,0,0)|^2}$ represents the Hilbert-Schmidt distance between the Bloch states at $\pm k$ [6,9].

The other exotic object is the nonlocal kernel $K^\rho(x,y) = (1/N_x)\sum_{k\sigma}[(1+2\rho_\sigma)/((1+\rho_\sigma)^2)]|u_k(\sigma)|^2 e^{ik(x-y)}$. Because of gain saturation, the effective gain depends on the occupation of the sites within a unit cell. The nonlocality of this expression could result in an imaginary part of the dispersion of $\bar\psi$ at the linear level. For the diamond chain, however, $K^\rho(x,y) = \delta_{xy}\sum_\sigma\{[1+2\rho_\sigma]/[(1+\rho_\sigma)^2]\}|u_0(\sigma)|^2$ is local and we can define the effective linear gain constant $\bar P = PK^\rho(x,x)$. In the following, we no longer consider the original field and drop the bar from $\bar\psi$.

Lasing state and Bogoliubov modes.—At this stage, we simply rewrote the CGLE projected onto the lowest band. We will now study the steady-state solution and its dynamical properties. Lasing will typically occur in the momentum state k_* that optimizes gain saturation [minimizing $\Lambda(k,k,k)$] and density uniformity. In the case of the diamond chain, there exist two such (equivalent [31]) momenta, 0 and π, and we will assume that $k_* = 0$ is spontaneously selected. The lasing steady state then reads

$$\psi_x(t) = \sqrt{n_0}e^{-i\omega_0 t}, \tag{10}$$

with $n_0 = n_S(\bar P - \gamma)/(P\Lambda_0)$ the density of the field, $\omega_0 = -2J + \alpha(\bar P + P\Lambda_0^\rho n_0/n_S)/2$ the laser frequency and the shortcut $\Lambda_0^\rho \equiv \Lambda^\rho(0,0,0)$.

We now consider the collective modes on top of the steady-state by perturbing it as $\psi_x(t) = e^{-i\omega_0 t}(\sqrt{n_0} + \sum_k \delta\psi_k(t)e^{ikx})$. These fluctuations obey the equation of motion

$$\begin{aligned} i\partial_t\delta\psi_k = &-i\frac{\Gamma}{2}(1-i\alpha)[(2\Lambda^\rho(0,k,0) - \Lambda_0^\rho)\delta\psi_k \\ &+\Lambda^\rho(k,0,0)\delta\psi^*_{-k}], \end{aligned} \tag{11}$$

where $\Gamma = Pn_0/n_S$ determines the relaxation rate for density fluctuations. As previously noticed in the atomic BEC context [6,9], where $\rho_\sigma = 0$ (two-body interactions), the quantities $\Lambda^0(0,k,0) = \sum_\sigma |u_k(\sigma)|^2|u_0(\sigma)|^2$ and $\Lambda^0(k,0,0) = \sum_\sigma u_k^*(\sigma)u^*_{-k}(\sigma)u_0^2(\sigma)$ are related to the quantum metric of the Bloch states; $\sqrt{1-|\Lambda^0(k,0,0)|^2}$ is also called the "condensate quantum distance." We remark that, as a further improvement over these works, we did not invoke any uniform-density assumption, and considered general nonlinearity functionals.

One can turn Eq. (11) into a 2×2 eigenproblem and find the complex eigenvalues $\omega_\pm(k)$. At $k = 0$, the phase (or Goldstone) mode has always $\omega_+ = 0$, reflecting the invariance of the dynamics under global phase shifts.

For the diamond chain, we have $\rho_B = \rho_C = \rho_A/2$ and $\Lambda^\rho(0,k,0) = \Lambda_0^\rho = \{1/[4(1+\rho_A)^2]\} + \{1/[8(1+\rho_B)^2]\}$, yielding

$$\omega_\pm(k) = -\frac{i}{2}\Gamma\Lambda_0 \pm \frac{\Gamma}{2}\sqrt{\alpha^2\Lambda_0^2 - (1+\alpha^2)\Lambda(k,0,0)^2 + i0^+}. \tag{12}$$

At small momentum, one can expand $\Lambda^\rho(k,0,0) \simeq \Lambda_0^\rho - (\beta/2)k^2$, where $\beta = \{1/[8(1+\rho_B)^2]\}$ plays the role of a metric. We thus recover a diffusive behavior for the Goldstone branch

$$\omega_+(k) \simeq -\frac{i}{4}\beta\Gamma(1+\alpha^2)k^2. \tag{13}$$

For exciton polaritons in dispersive bands [32,33], the Goldstone branch diffuses as $\omega_+(k) \simeq 2iJ\alpha k^2$. In contrast, Eq. (13) features the geometric quantity β, but also a peculiar functional dependence on Γ, α. In particular, α enters at the quadratic level instead of linearly, suggesting that the modulational instabilities (that appear for $J\alpha > 0$ in the dispersive case [25,34,35]) are tamed by the quantum geometry. We confirm this important statement in [36], which may have an important impact on applications. The stability of the flat-band laser in the case of slow reservoir dynamics $\gamma_R \sim \gamma$, as well as the validity regime of the projected model, are also investigated in [36].

Fate of the KPZ nonlinearity.—So far, we have been dealing with deterministic evolution and small perturbations. We now supplement the CGLE (3) with a stochastic drive $\sqrt{D}\xi_x(t)$, where D is the strength of the noise and ξ is taken as an uncorrelated random variable of zero mean and unit variance, $\langle\xi^*_{x\sigma}(t)\xi_{x'\sigma'}(t')\rangle = \delta_{xx'}\delta_{\sigma\sigma'}\delta(t-t')$. Since H_0 is Hermitian and the Bloch states are orthogonal, the noise variance is unaffected by the projection onto the lowest band (no Petermann broadening is introduced [38]); hence, one can simply complement the projected CGLE (7) with a white noise term $\sqrt{D}\xi_x(t)$ of unit variance.

Because of the absence of long-range order, Bogoliubov theory in low dimensions is not fully consistent and its conclusions have to be taken with a grain of salt. In 1D nonequilibrium systems, it has been theoretically [13–15] and experimentally [16] established that the low-energy dynamics is dominated by phase fluctuations, as described by the KPZ equation [39]

$$\partial_t\phi = \nu\nabla^2\phi + \lambda(\nabla\phi)^2 + \sqrt{\mathcal{D}}\xi_\phi, \tag{14}$$

where $\langle\xi_\phi(xt)\xi_\phi(x't')\rangle = \frac{1}{2}\delta(x-x')\delta(t-t')$. The KPZ nonlinearity of strength λ distinguishes this growth equation from the linear Gaussian evolution. In the physics of interfaces, the Laplacian describes surface tension favoring a smooth interface, while the nonlinear term entails that growth occurs in the direction locally normal to the

interface. While the exponential decay of the spatial correlations is unaffected by $\lambda \neq 0$, the hallmark of KPZ physics concerns the dynamical exponent characterizing the decay of temporal correlations.

KPZ physics was identified in the context of polariton wires [40], where the linear kinetic term is nonlocal and the nonlinear term is local. In contrast, Eq. (7) features a *nonlocal and nonlinear* term. To go beyond Bogoliubov theory, we adopt the density-phase formalism $\psi(x,t) = \sqrt{n_0+\delta n}e^{-i\omega_0 t+i\phi}$, where we only require the density fluctuations to be small. Treating x as a continuous variable, we then divide both sides of Eq. (7) by $e^{i\phi(x)}$ and expand

$$e^{i[\phi(y_2)+\phi(y_3)-\phi(y_1)-\phi(x)]} \simeq 1 + i\nabla\phi(x)(z_2+z_3-z_1) + \frac{i}{2}\nabla^2\phi(x)(z_2^2+z_3^2-z_1^2) - \frac{1}{2}[\nabla\phi(x)]^2(z_2+z_3-z_1)^2.$$

In principle, one can also perform a Taylor expansion for density fluctuations, but it turns out that the spatial derivatives of the density will eventually yield higher-order corrections to the phase equation. For instance, the Laplacian $\nabla^2\delta n$ will generate a term $\nabla^4\phi$. Physically, this is related to the fact that density correlations are very short ranged. We then approximate $\delta n(y_j) \simeq \delta n(x)$; note that one also drops $\nabla\delta n, \nabla^2\delta n$ in the case of dispersive bands.

We have reduced the problem to evaluating moments of the quantum geometric kernel

$$\int dz_j\, dk_j\, e^{ik_1z_1-ik_2z_2-ik_3z_3}\Lambda^\rho(k_1,k_2,k_3)\mathrm{Pol}(z_1,z_2,z_3), \quad (15)$$

where $\mathrm{Pol}(z_1,z_2,z_3)$ denotes a polynomial with real coefficients. In the case of the diamond chain, one explicitly verifies that $\Lambda^\rho(k_1,k_2,k_3) = \Lambda^\rho(-k_1,-k_2,-k_3)$. This entails that only even polynomials survive the integration and the result is real. It is easy to recognize that integration of $z_2^2+z_3^2-z_1^2$ yields $(d^2/dk^2)\Lambda^\rho(k,0,0) = -\beta$, while the coefficient $\eta = -(\partial_{k_2}+\partial_{k_3}-\partial_{k_1})^2\Lambda^\rho(k_1,k_2,k_3)|_{k_j=0} = 2\beta$ stems in front of $(\nabla\phi)^2$. Putting pieces together and separating real and imaginary parts of the CGLE, we finally arrive at the density-phase equations

$$\partial_t\delta n = -\Gamma\Lambda_0^\rho\delta n + \frac{\alpha\beta}{2}\Gamma n_0\nabla^2\phi + \frac{\Gamma}{2}n_0\eta(\nabla\phi)^2 + 2\sqrt{n_0 D}\xi_n,$$
$$\partial_t\phi = \frac{\alpha\Gamma}{2}\Lambda_0^\rho\frac{\delta n}{n_0} + \frac{\Gamma}{4}\beta\nabla^2\phi - \frac{\alpha\Gamma}{4}\eta(\nabla\phi)^2 + \sqrt{\frac{D}{n_0}}\xi_\phi, \quad (16)$$

where we now have two uncorrelated sources of noise, $\langle\xi_\phi(xt)\xi_\phi(x't')\rangle = \frac{1}{2}\delta(x-x')\delta(t-t')$ and $\langle\xi_n(xt)\xi_n(x't')\rangle = \frac{1}{2}\delta(x-x')\delta(t-t')$. The last step consists in adiabatically tracing out density fluctuations, so to be left with the equation for the low-energy phase dynamics

$$\partial_t\phi = \frac{\beta}{4}\Gamma(1+\alpha^2)\nabla^2\phi + \sqrt{\frac{D}{n_0}(1+\alpha^2)}\xi_\phi. \quad (17)$$

Remarkably, the KPZ nonlinearity is zero because of an exact cancellation of the $(\nabla\phi)^2$ term, which could have potentially been generated by interactions and Bloch geometry. Also, notice that the coefficient of the Laplacian recovers the diffusion of the Goldstone mode in Eq. (13) and the noise coefficient is the square root of the Henry-Schawlow-Townes linewidth per unit length [41].

This argument for the cancellation of the KPZ nonlinearity holds irrespective of the dimensionality of the system, but it is of particular relevance in on dimension, where the renormalization group (RG) applied to the KPZ equation predicts that the Gaussian fixed point is unstable. Then, in principle, the RG flow may regenerate an effective KPZ nonlinearity originating from higher order corrections. Hence, we now aim at numerically testing the validity of our results by studying the presence of KPZ effects in the correlation functions. We ran extensive simulations of the *full unprojected* CGLE (3), including a stochastic drive, with an initial seed chosen to lase at $k = 0$. We computed the first-order coherence function, defined by the statistical averages in the steady state

$$g^{(1)}(x,t) = \langle a_x^*(t)a_0(0)\rangle. \quad (18)$$

The hallmark of KPZ is a decay of temporal correlations of the form $g^{(1)}(0,t) \sim \exp(-\mathcal{A}t^{2/3})$, with some nonuniversal constant $\mathcal{A}$. In Fig. 2, we plot $-\log g^{(1)}(0,t)$ for different system sizes and values of g, showing no sign of the $2/3$ KPZ exponent.

On the other hand, Eq. (17) has the form of a Gaussian process, described by the Edwards-Wilkinson (EW) equation $\partial_t\phi = \nu\nabla^2\phi + \sqrt{\mathcal{D}}\xi_\phi$. The correlations for this model can be easily computed; in one dimension, they read $g^{(1)}_{\mathrm{EW}}(0,t) = n_0\exp[-(\mathcal{D}/4)\sqrt{(t/\pi\nu)}]$ and $g^{(1)}_{\mathrm{EW}}(x,0) = n_0\exp[-(\mathcal{D}/8\nu)x]$. While these are the predictions for an infinite system, in general there will be finite size corrections. In particular, at large times, we expect the Schawlow-Townes (ST) exponential decay $g^{(1)}_{\mathrm{ST}}(0,t) = n_0\exp[-(\mathcal{D}/4N_x)t]$, with a linewidth inversely proportional to the system size [42]. We recall that the linewidth is also very sensitive to the presence of KPZ physics, with a scaling $\sim N_x^{-1/2}$, which can already show up for a dozen of resonators [41]. The EW and ST predictions are also plotted in Fig. 2 and match perfectly the numerical data, confirming the validity of Eq. (17) and the absence of KPZ physics for all numerically accessible system sizes. (The small discrepancy at small times is due to high-energy fluctuations, for which density cannot be eliminated).

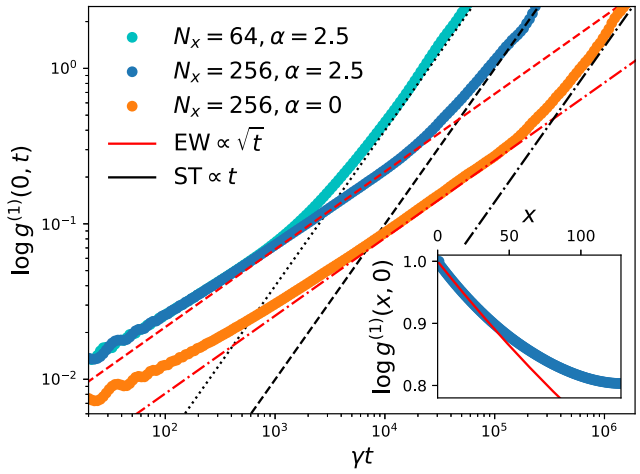

FIG. 2. Correlation functions computed solving numerically Eq. (3) plus a stochastic drive. (main) The temporal correlation function $g^{(1)}(0,t)$, displaying a crossover from Edwards-Wilkinson to Schawlow-Townes, and no sign of KPZ. The two EW red lines correspond to $\alpha = 0$ (red dashed-dotted) and $\alpha = 2.5$ (red dashed), while the ST decay depends also on the size of the system (black dashed dotted line for $\alpha = 0$, $N_x = 256$, dashed for $\alpha = 2.5$, $N_x = 256$, and dotted for $\alpha = 2.5$, $N_x = 64$). (inset) Decay of $g^{(1)}(x,0)$, with initial slope predicted by EW (before finite-size effects set in). We take as parameters $P = 2\gamma$, $n_S = 250$, $D = 2\gamma$, $J = 5\gamma$.

Generalizations.—To better understand under which conditions the KPZ term exactly cancels, we introduce a photon-photon interaction term $g|\psi_{x\sigma}|^2\psi_{x\sigma}$ in Eq. (3), and set $\alpha = 0$. In this case, the real and imaginary parts of the nonlinearity have different functional forms. As a consequence, the projected CGLE (7) contains an extra term $g\sum_{y_1y_2y_3} K^0(x,y_1,y_2,y_3)\bar{\psi}^*_{y_1}\bar{\psi}_{y_2}\bar{\psi}_{y_3}$, since dealing with the cubic nonlinearity is equivalent to setting $\rho_\sigma = 0$. The derivation of the Bogoliubov modes and of the density-phase equations follows straightforwardly. Eliminating the density, the final phase equation reads

$$\partial_t\phi = \frac{\Gamma}{4}\left\{\beta + \frac{\Lambda^0}{\Lambda^\rho}\beta^0\left(\frac{2\mu}{\Gamma}\right)^2\right\}\nabla^2\phi + \frac{\mu}{2}\left\{\eta_0 - \frac{\Lambda^0}{\Lambda^\rho}\eta\right\}(\nabla\phi)^2 + \sqrt{\frac{D}{n_0}(1+\alpha^2)}\xi_\phi, \quad (19)$$

where we defined the blueshift $\mu = gn_0$. This is a proper KPZ equation, provided that $\mu \neq 0$ and $\eta_0\Lambda^\rho \neq \Lambda^0\eta$. We have thus demonstrated that, in a flat-band laser, a KPZ term of geometric origin can be present under a few assumptions: first, the presence of a nontrivial Bloch geometry; second, the real and imaginary part of the nonlinearity should not be proportional to each other, and, in particular, the real part must be nonzero; third, the density of the lasing steady-state has to be nonuniform, otherwise all the ρ_σ would be the same and $(\eta^0/\eta^\rho) = (\Lambda^0/\Lambda^\rho) = (1+\rho_\sigma)^2$. In particular, this last statement implies that the *uniform-pairing condition* [8,9,43] always entails a cancellation of the KPZ nonlinearity. These requirements have no analog in dispersive systems, where the KPZ nonlinearity is simply proportional to the bandwidth, and where the real nonlinearity is not required to produce KPZ physics. In practice, the KPZ contribution is quantitatively small, and we did not manage to isolate it numerically with the available computational resources (the KPZ nonlinearity is absent for $\mu = 0$, and the Laplacian term dominates for large μ).

Concluding remarks.—We have revealed how gain competition can stabilize lasing in flat bands with nontrivial Bloch geometry. This phenomenon occurs despite the fact that no mode is privileged at the linear level.

We have computed the Bogoliubov spectrum and the peculiar diffusion coefficient of the corresponding Goldstone branch, which shows resilience against the modulational instability present in the dispersive case [25,34,35]. This suggests that quantum geometry may have an impact in applications, allowing for more stable laser arrays. Similarly, a KPZ nonlinearity can arise from geometric effects, but it is exactly cancelled in the relevant cases of *uniform pairing* or whenever the real part of the nonlinearity is zero or proportional to its imaginary part. This suggests that the KPZ nonlinearity is typically small in practice. Our analytical results, obtained under weak assumptions, were numerically validated using the diamond chain.

Previous works based on the Lieb chain [25] considered a nonuniform gain to induce lasing in a flat band, which led to a momentum-dependent gain $P(k) = P_0 - P_2k^2 + \cdots$ at the linear level determined by the shape of the Bloch states. In that case, a KPZ nonlinear term proportional to P_2 is known to appear in the equation for the phase [14]. A similar scenario occurs in topological lasers [11,42], but with a weakly dispersive edge mode. Instead, in this Letter we have considered bands that are flat in both their real and imaginary part, which led to a cancellation of the KPZ term.

We notice that a PT-symmetric flatband laser was proposed in [17] and a Kagome polariton condensate was realized in [18], without analyzing the role of quantum geometry. In both these cases, the flat band is not gapped from the dispersive bands, such that our projected theory does not apply. It would be interesting to assess the presence of the KPZ nonlinearity in these cases, as well as in settings displaying flat-band skin effects [44].

Here we limited ourselves to a semiclassical theory, where interactions are weak enough to approximate the field on each site by a coherent state. It would be of great interest to investigate the quantum regime of strong interactions and explore flat band physics in quantum dissipative systems. Experimental platforms like circuit QED promise to be very well suited for this purpose [30,45]. We remark that clean samples are needed, since flat bands are particularly sensitive to disorder [12].

All numerical calculations were performed using the Julia Programming Language [46].

We are grateful to Daniele De Bernardis, Maxime Burgher, Sebastian Diehl, and Stefano Longhi for stimulating discussions and exchanges. This research was financially supported by the ERC grant LATIS, the EOS project CHEQS, and the FRS-FNRS (Belgium). Computational resources have been provided by the Consortium des Équipements de Calcul Intensif (CÉCI), funded by the Fonds de la Recherche Scientifique de Belgique (FRS-FNRS) under Grant No. 2.5020.11 and by the Walloon Region.

[1] R. Bistritzer and A. H. MacDonald, Moiré bands in twisted double-layer graphene, Proc. Natl. Acad. Sci. U.S.A. **108**, 12233 (2011).
[2] Y. Cao, V. Fatemi, S. Fang, K. Watanabe, T. Taniguchi, E. Kaxiras, and P. Jarillo-Herrero, Unconventional superconductivity in magic-angle graphene superlattices, Nature (London) **556**, 43 (2018).
[3] Y. Cao, V. Fatemi, A. Demir, S. Fang, S. L. Tomarken, J. Y. Luo, J. D. Sanchez-Yamagishi, K. Watanabe, T. Taniguchi, E. Kaxiras, R. C. Ashoori, and P. Jarillo-Herrero, Correlated insulator behaviour at half-filling in magic-angle graphene superlattices, Nature (London) **556**, 80 (2018).
[4] S. D. Huber and E. Altman, Bose condensation in flat bands, Phys. Rev. B **82**, 184502 (2010).
[5] S. Takayoshi, H. Katsura, N. Watanabe, and H. Aoki, Phase diagram and pair Tomonaga-Luttinger liquid in a Bose-Hubbard model with flat bands, Phys. Rev. A **88**, 063613 (2013).
[6] A. Julku, G. M. Bruun, and P. Törmä, Quantum geometry and flat band Bose-Einstein condensation, Phys. Rev. Lett. **127**, 170404 (2021).
[7] S. Peotta and P. Törmä, Superfluidity in topologically nontrivial flat bands, Nat. Commun. **6**, 8944 (2015).
[8] K.-E. Huhtinen, J. Herzog-Arbeitman, A. Chew, B. A. Bernevig, and P. Törmä, Revisiting flat band superconductivity: Dependence on minimal quantum metric and band touchings, Phys. Rev. B **106**, 014518 (2022).
[9] A. Julku, G. Salerno, and P. Törmä, Superfluidity of flat band Bose-Einstein condensates revisited, Low Temp. Phys. **49**, 701 (2023).
[10] W. Noh, H. Nasari, H.-M. Kim, Q. Le-Van, Z. Jia, C.-H. Huang, and B. Kanté, Experimental demonstration of single-mode topological valley-Hall lasing at telecommunication wavelength controlled by the degree of asymmetry, Opt. Lett. **45**, 4108 (2020).
[11] A. Loirette-Pelous, I. Amelio, M. Seclì, and I. Carusotto, Linearized theory of the fluctuation dynamics in two-dimensional topological lasers, Phys. Rev. A **104**, 053516 (2021).
[12] F. Baboux, L. Ge, T. Jacqmin, M. Biondi, E. Galopin, A. Lemaître, L. Le Gratiet, I. Sagnes, S. Schmidt, H. E. Türeci, A. Amo, and J. Bloch, Bosonic condensation and disorder-induced localization in a flat band, Phys. Rev. Lett. **116**, 066402 (2016).
[13] K. Ji, V. N. Gladilin, and M. Wouters, Temporal coherence of one-dimensional nonequilibrium quantum fluids, Phys. Rev. B **91**, 045301 (2015).
[14] L. He, L. M. Sieberer, E. Altman, and S. Diehl, Scaling properties of one-dimensional driven-dissipative condensates, Phys. Rev. B **92**, 155307 (2015).
[15] D. Squizzato, L. Canet, and A. Minguzzi, Kardar-Parisi-Zhang universality in the phase distributions of one-dimensional exciton-polaritons, Phys. Rev. B **97**, 195453 (2018).
[16] Q. Fontaine, D. Squizzato, F. Baboux, I. Amelio, A. Lemaître, M. Morassi, I. Sagnes, L. L. Gratiet, A. Harouri, M. Wouters, I. Carusotto, A. Amo, M. Richard, A. Minguzzi, L. Canet, S. Ravets, and J. Bloch, Kardar-Parisi-Zhang universality in a one-dimensional polariton condensate, Nature (London) **608**, 687 (2022).
[17] S. Longhi, Photonic flat-band laser, Opt. Lett. **44**, 287 (2019).
[18] T. H. Harder, O. A. Egorov, C. Krause, J. Beierlein, P. Gagel, M. Emmerling, C. Schneider, U. Peschel, S. Höfling, and S. Klembt, Kagome flatbands for coherent exciton-polariton lasing, ACS Photonics **8**, 3193 (2021).
[19] G. Harari, M. A. Bandres, Y. Lumer, M. C. Rechtsman, Y. D. Chong, M. Khajavikhan, D. N. Christodoulides, and M. Segev, Topological insulator laser: Theory, Science **359**, eaar4003 (2018).
[20] A. Amo and J. Bloch, Exciton-polaritons in lattices: A nonlinear photonic simulator, C.R. Phys. **17**, 934 (2016).
[21] M. Grabherr, M. Miller, R. Jager, R. Michalzik, U. Martin, H. Unold, and K. Ebeling, High-power VCSELs: Single devices and densely packed 2-D-arrays, IEEE J. Sel. Top. Quantum Electron. **5**, 495 (1999).
[22] I. Carusotto and C. Ciuti, Quantum fluids of light, Rev. Mod. Phys. **85**, 299 (2013).
[23] C. Henry, Theory of the linewidth of semiconductor lasers, IEEE J. Quantum Electron. **18**, 259 (1982).
[24] S. Longhi, Y. Kominis, and V. Kovanis, Presence of temporal dynamical instabilities in topological insulator lasers, Europhys. Lett. **122**, 14004 (2018).
[25] F. Baboux, D. D. Bernardis, V. Goblot, V. N. Gladilin, C. Gomez, E. Galopin, L. L. Gratiet, A. Lemaître, I. Sagnes, I. Carusotto, M. Wouters, A. Amo, and J. Bloch, Unstable and stable regimes of polariton condensation, Optica **5**, 1163 (2018).
[26] J. Vidal, B. Douçot, R. Mosseri, and P. Butaud, Interaction induced delocalization for two particles in a periodic potential, Phys. Rev. Lett. **85**, 3906 (2000).
[27] M. Hafezi, E. A. Demler, M. D. Lukin, and J. M. Taylor, Robust optical delay lines with topological protection, Nat. Phys. **7**, 907 (2011).
[28] M. A. Bandres, S. Wittek, G. Harari, M. Parto, J. Ren, M. Segev, D. N. Christodoulides, and M. Khajavikhan, Topological insulator laser: Experiments, Science **359**, eaar4005 (2018).
[29] S. Klembt, T. Harder, O. Egorov, K. Winkler, R. Ge, M. Bandres, M. Emmerling, L. Worschech, T. Liew, M. Segev *et al.*, Exciton-polariton topological insulator, Nature (London) **562**, 552 (2018).
[30] J. G. C. Martinez, C. S. Chiu, B. M. Smitham, and A. A. Houck, Flat-band localization and interaction-induced delocalization of photons, Sci. Adv. **9**, eadj7195 (2023).

[31] The symmetry operation $a_j \to (-1)^j a_j, b_j \to -(-1)^j c_j$, $c_j \to (-1)^j b_j$ preserves both H_0 of the π-flux diamond chain and the nonlinearity, while mapping momentum k into $k + \pi$.

[32] M. H. Szymańska, J. Keeling, and P. B. Littlewood, Nonequilibrium quantum condensation in an incoherently pumped dissipative system, Phys. Rev. Lett. **96**, 230602 (2006).

[33] M. Wouters and I. Carusotto, Excitations in a nonequilibrium Bose-Einstein condensate of exciton polaritons, Phys. Rev. Lett. **99**, 140402 (2007).

[34] N. Bobrovska, E. A. Ostrovskaya, and M. Matuszewski, Stability and spatial coherence of nonresonantly pumped exciton-polariton condensates, Phys. Rev. B **90**, 205304 (2014).

[35] N. Bobrovska and M. Matuszewski, Adiabatic approximation and fluctuations in exciton-polariton condensates, Phys. Rev. B **92**, 035311 (2015).

[36] See Supplemental Material at http://link.aps.org/supplemental/10.1103/PhysRevLett.132.186902 for a comparison of the Bogoliubov modes between the full and projected models, and the stability diagram for a nonadiabatic reservoir dynamics. See also Ref. [37] therein.

[37] M. Seclì, T. Ozawa, M. Capone, and I. Carusotto, Spatial and spectral mode-selection effects in topological lasers with frequency-dependent gain, APL Photonics **6**, 050803 (2021).

[38] I. Amelio and I. Carusotto, Bogoliubov theory of the laser linewidth and application to polariton condensates, Phys. Rev. A **105**, 023527 (2022).

[39] M. Kardar, G. Parisi, and Y.-C. Zhang, Dynamic scaling of growing interfaces, Phys. Rev. Lett. **56**, 889 (1986).

[40] V. N. Gladilin, K. Ji, and M. Wouters, Spatial coherence of weakly interacting one-dimensional nonequilibrium bosonic quantum fluids, Phys. Rev. A **90**, 023615 (2014).

[41] I. Amelio, A. Chiocchetta, and I. Carusotto, Kardar-Parisi-Zhang universality in the coherence time of nonequilibrium one-dimensional quasicondensates, Phys. Rev. E **109**, 014104 (2024).

[42] I. Amelio and I. Carusotto, Theory of the coherence of topological lasers, Phys. Rev. X **10**, 041060 (2020).

[43] M. Tovmasyan, S. Peotta, P. Törmä, and S. D. Huber, Effective theory and emergent SU(2) symmetry in the flat bands of attractive Hubbard models, Phys. Rev. B **94**, 245149 (2016).

[44] C. Martinez-Strasser, M. A. J. Herrera, A. Garcia-Etxarri, G. Palumbo, F. K. Kunst, and D. Bercioux, Topological properties of a non-Hermitian quasi-1D chain with a flat band, Adv. Quantum Technol. **7**, 2300225 (2024).

[45] A. R. Kolovsky, P. S. Muraev, and S. Flach, Conductance transition with interacting bosons in an Aharonov-Bohm cage, Phys. Rev. A **108**, L010201 (2023).

[46] J. Bezanson, A. Edelman, S. Karpinski, and V. B. Shah, Julia: A fresh approach to numerical computing, SIAM Rev. **59**, 65 (2017).